DOI: 10.1002/ejic.201100261

Ultrasound-Induced Rapid Intercalation of Biselenite in Layered Double Hydroxides

Jong Hyeon Lee,[a] Yeon Soo Lee,[b] Hana Kim,[b] and Duk-Young Jung*[b]

Keywords: Clays / Layered compounds / Layered double hydroxides / Ion exchange / Selenium / Intercalations / Decarbonation

The deintercalation of carbonate (CO_3^{2-}) ions from MgAl-layered double hydroxides (LDHs) (Mg/Al = 2) both in monolayer films and powdered samples under atmospheric conditions in ethanol was investigated. A selenous acid precursor was incorporated into the interlayer gallery. Treatment with 0.5 M selenous acid (H_2SeO_3) for 30 min with powdered LDHs or with 0.1 M H_2SeO_3 for 5 min with the thin film LDHs resulted in carbonate ions being exchanged with biselenite ($HSeO_3^-$) ions. Electron microscopy showed that the morphologies of the original LDH particles remained after the reaction, despite the ultrasound being continuously applied for up to 2 h. XRD, FTIR and Raman spectroscopic scattering results strongly suggested that cyclic dimers of biselenite ions were incorporated into the gallery spaces of the LDHs, vertically arranged to the horizontal axes of the MgAl-LDH layers.

Introduction

Layered double hydroxides (LDHs), also known as hydrotalcite-like clays, have potential uses as catalysts, ion-exchangers, separators and scavengers of hazardous anionic contaminants.[1–6] They consist of layers of positively charged metal hydroxides, interlayer anions and water molecules represented by the general formula $[M^{2+}_{(1-x)}M^{3+}_x(OH)_2]A^{n-}_{x/n}\cdot mH_2O$, where M^{2+} and M^{3+} are divalent and trivalent metal ions, respectively, capable of occupying the octahedral holes of Brucite-like layers and A^{n-} is a virtually hydrated exchangeable anion positioned in the gallery spaces between layers.[7–9] LDHs can participate in anion-exchange reactions and incorporate various anions, such as inorganic anions (carbonate, nitrate, chloride etc.), carboxylates, oxometallates, sulfates/sulfonate, selenite/selenate and amino acids.[3–6]

Since carbonate (CO_3^{2-}) has an exceptionally high affinity for hydrotalcite-like clays, crystalline LDHs possessing carbonate ions in the interlayer gallery spaces (LDH-carbonate) are typically obtained but other anions are not readily incorporated. Recent developments in the intercalation chemistry of LDHs have focused on the preparation of crystalline LDHs containing exchangeable anions by means of decarbonation of LDH-carbonate with dilute HCl[10] or acetate buffer[11] systems. However, the strong acidity of HCl and the fast infiltration of atmospheric carbon dioxide in aqueous solution require controlled use of the acid and an inert atmosphere during reaction. Exchange reactions involve an equilibration of water-soluble anions out of the intercalated LDHs − reaction times of longer than 24 h and continuous agitation are generally needed to produce crystalline LDHs with ions other than carbonate. Therefore, there is much scope for the expediting of intercalation methods.

Most investigations of LDH reactions have been on those performed in aqueous solutions with water-soluble anions as guest molecules.[12,13] Reactions in aqueous systems involve the equilibrium of partial dissolution and recrystallisation through the hydrolysis of LDH host layers which hampers the formation of LDHs containing specific anions with controlled crystal sizes and high crystallinity. In intercalation chemistry, the adsorption of anions onto the hydroxide surfaces of LDHs is strongly governed by either ionic or hydrogen bonding between the incoming guest molecules and the LDH host layers. We have recently reported anisotropic 2D assemblies of LDH nanocrystals with good orientations on solid surfaces as an intercalation platform which provided the desired solvothermal anion-exchange reactions in ethanol/toluene mixed solutions with protic organic acids, such as linear dicarboxylic acid and poly(acrylic acid), as guest molecules.[14–18] In those studies, the small amount of alcohol enabled not only solubility of the organic acids but also space for high diffusion rates into the LDH interlayer space. The morphology of the LDH particles was found to be preserved after the reactions. The alcohol also led to partial deprotonation of the high pK_a poly(acrylic acid), suggesting that the alcohol could aid the reaction of various protic acids with low pK_a values under

[a] Department of Chemistry, The Catholic University of Korea, Bucheon, Gyeonggi, 420-743, Korea
[b] Department of Chemistry and Sungkyunkwan Advanced Institute of Nanotechnology, Institute of Basic Sciences, Sungkyunkwan University, Suwon 440-746, South Korea
Fax: +82-31-290-7075
E-mail: dyjung@skku.edu

atmospheric conditions. Solvothermal anion-exchange of LDHs was conducted above 100 °C, possibly leading to defects in the crystal structure and deformation of the LDHs' particle shapes when large amounts of protic organic solvents, e.g. alcohols, were used. Thus, investigation of less intrusive anion exchange in bulk LDH-carbonates using organic systems was undertaken to obtain crystalline LDHs containing ions other than carbonate.

Here, we investigated the use of ultrasound-assisted intercalation[19] of selenous acid (H_2SeO_3) through the substitution of carbonate ions between the layers of LDHs using ethanol as a protic reaction medium. The intercalation reaction was investigated for LDH powders and well-oriented LDH nanocrystals on a silicon substrate, giving information about the molecular orientation of the intercalated anions and allowing observation of the changes of crystal thickness perpendicular to the substrate plane. The LDHs dissolve a little in alcoholic media and the carbonate ions were successfully exchanged with biselenite ions in the form of cyclic dimers. Samples were analysed by FTIR and Raman scattering spectroscopy, chemical analysis and elemental mapping to monitor the deintercalation of carbonate ions and the intercalation of biselenite dimers (Scheme 1).

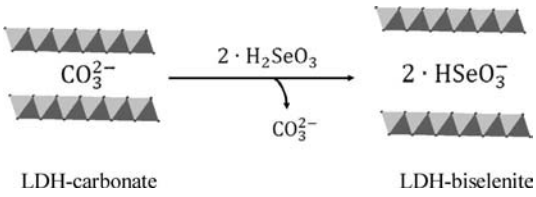

Scheme 1. Carbonate exchange reaction with H_2SeO_3 in the LDH interlayer space.

Results and Discussion

Figure 1 shows scanning electron microscopy (SEM) images of LDH-carbonate powder samples with diameters ranging from 100 to 500 nm and thicknesses of ca. 100 nm. The monolayer assemblies of LDH-carbonate crystals obtained by sonication of the Si substrates were highly oriented. The LDH-carbonate crystals on the Si substrate showed highly anisotropic arrays when compared with structures resulting from simple solvent evaporation of a colloidal suspension. The bonding between the LDH and the Si wafer can be ascribed to electrostatic attraction resulting from positively charged LDH particles and the negatively charged Si substrate.[14–18] Topotactic exchange of CO_3^{2-} with $HSeO_3^-$ in the gallery space of the LDHs occurred in a 100 mM selenous acid/ethanol solution assisted by ultrasound. The SEM image of the LDH-biselenite shows that the lateral positions and the lateral size of the LDH crystals were unchanged. However, the heights of the LDH nanocrystals along the crystallographic *c* axis were considerably expanded.

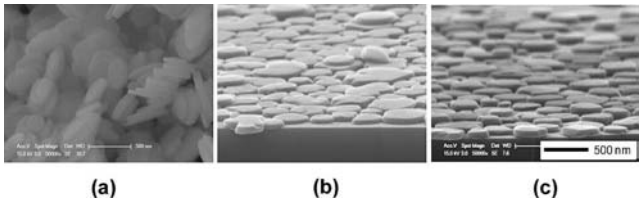

Figure 1. Typical SEM images of (a) the pristine LDH-carbonate powder sample (b) monolayer assembly of LDH-carbonate film on Si prepared in 1-butanol and (c) LDH-biselenite on Si prepared by ultrasound treatment in 100 mM H_2SeO_3 in ethanol for 5 min.

X-ray Diffraction (XRD) Analysis of LDH-Biselenite Films and Powders

XRD patterns of the LDH-carbonate on the Si substrate and the product obtained after biselenite exchange are shown in Figure 2. The LDH-biselenite sample was prepared through anion-exchange of the LDH-carbonate film with 100 mM selenous acid in ethanol assisted by ultrasound for 5 min at room temperature. The LDH-carbonate films exhibited only strong (*00l*) reflections, indicating highly orientated LDH crystals along the crystallographic *c* axis perpendicular to the substrate plane. The low-angle reflection appearing at 11.6°/2θ (d = 7.6 Å) corresponds to the interlayer spacing of the LDHs-carbonate. The peaks of the pristine LDH-carbonate disappeared after reacting for 5 min, though their (*00l*) orientation was maintained in the preferred crystallographic orientation of the LDH-biselenite, implying that biselenite successfully exchanged with the carbonate ions in the gallery space between the LDH layers and that the LDH-biselenite crystals consisted of stacked LDH sheets with interlayer spaces being filled by highly oriented structures. The low intensity of the peak at 11.6°/2θ corresponds to residual unreacted LDH-carbonate. The d value of 11.5 Å was much larger than that of 8.1 Å re-

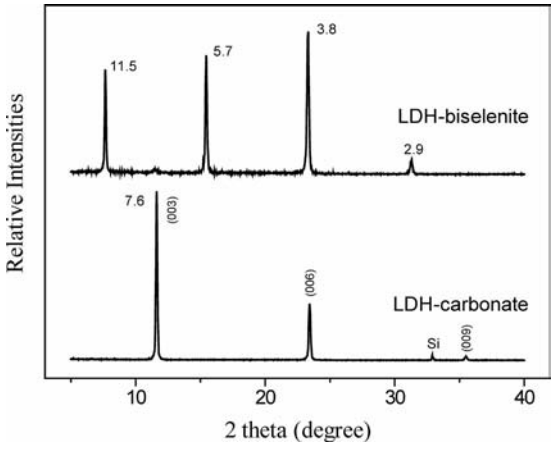

Figure 2. XRD patterns and basal spacings [Å] of LDH-carbonate and LDH-biselenite prepared on Si (*100*) substrates. The LDH-biselenite film was prepared by applying ultrasound for 5 min in 100 mM H_2SeO_3 in ethanol. The peak around 32.9° displayed by the LDH-carbonate is characteristic of the (*200*) plane of the Si substrate. The peak around 11.6° displayed by the LDH-biselenite was ascribed to residual LDH-carbonate. The intensity of the XRD spectrum of LDH-biselenite was multiplied by 2 for comparison with that of LDH-carbonate.

ported for LDH-selenite prepared in an aqueous system with sodium selenite (Na_2SeO_3).[20] The large d value observed in this work was ascribed to the different molecular conformation of biselenite ions in the gallery space, partly due to interlayer hydrogen bonding with water molecules.

Biselenite incorporation in the LDH gallery space was strong because the basal spacing and lateral position of the crystals did not change after additional ultrasound treatment for up to 2 h. The solvation of selenous acid in alcohol[21] and the pre-swelling with alcohol[22] likely aided the rapid anion exchange. These results suggest that the current method is a powerful tool for the substitution of carbonate ions with biselenite ions, replacing one of the most strongly bound anions in the interlayer gallery of LDHs.[12] This method did not require the inert atmosphere employed in conventional LDH synthesis to prevent absorption of carbon dioxide.

Intercalations were investigated through XRD analysis of samples obtained from various concentrations of selenous acid reacted for 5 min (Figure 3). The intercalation of selenous acid in the gallery space of the LDH effectively exchanged the carbonates from the original LDH-carbonate. Five minutes was sufficient for ion exchange with an acid concentration of 100 mM. The low-angle XRD peak of the LDH-carbonate sample was dramatically decreased as the acid concentration increased (Figure 3, a). The peak intensities for the LDH-biselenite gradually increased as the acid concentrations increased, indicating that higher concentrations of selenous acid resulted in more rapid overall reaction with LDHs. At low concentrations (1 mM and 3 mM), the main XRD peaks of the LDH-carbonate were reduced and peak broadening occurred, likely due to the lower pK_a of selenous acid (pK_{a1} = 2.64 at 25 °C) compared with that of carbonic acid (pK_{a1} = 6.35 at 25 °C). There were no diffraction patterns assignable to other intercalated phases. Part b of Figure 3 details the peaks between 23 and 24°/2θ corresponding to the third harmonic of LDH-biselenite and to the second harmonic of LDH-carbonate. As the acid concentration increased, the peaks for LDH-carbonate shifted to lower angles and the characteristic biselenite-incorporated peak appeared. The inverse of intensity for the two first (*00l*) peaks in LDH-biselenite compared with LDH-carbonate is probably attributable to an increase in electron density in the mid-plane of the interlayers.[23–24]

Given the effective carbonate-exchange reaction of selenous acid with LDH-carbonate films on Si, a similar process was applied to powdered LDH-carbonate samples. The XRD results are shown in Figure 4. The powder XRD pattern of LDH-carbonate indicated a well-crystallised, rhombohedral, hydrotalcite-like, $3R_1$ phase indexed with lattice parameters of a = 3.04 Å ($a = 2d_{110}$) and c = 22.89 Å. The low angle reflection appearing at 11.58°/2θ (d = 7.63 Å) corresponded to the interlayer spacing of the LDH-carbonate with its higher harmonic appearing at 23.46°/2θ (d = 3.79 Å). Intercalation of biselenite between the LDH layers increased the basal spacing, similar to that observed in the LDH-biselenite films. The peak for LDH-biselenite

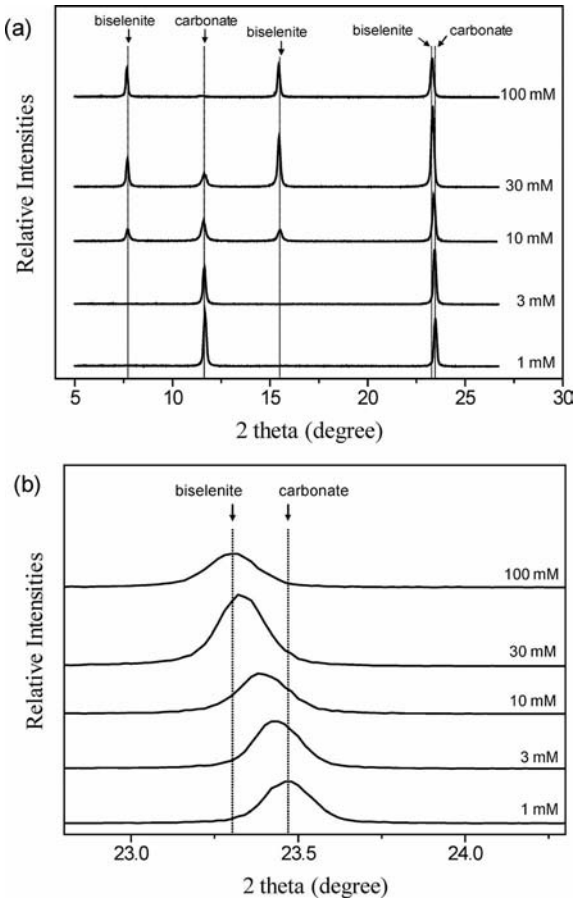

Figure 3. XRD patterns of LDH-biselenite films on Si substrates prepared by ultrasound treatment for 5 min under different concentrations of H_2SeO_3 in ethanol in (a) wide scan and (b) at around 23.5°.

emerged at ca. 7.9°/2θ, corresponding to a basal spacing of 11.2 Å. The broad peaks at ca. 30–50°/2θ emerged due to structural disorder arising from stacking faults. Reaction times of 30 min were sufficient to exchange the carbonate

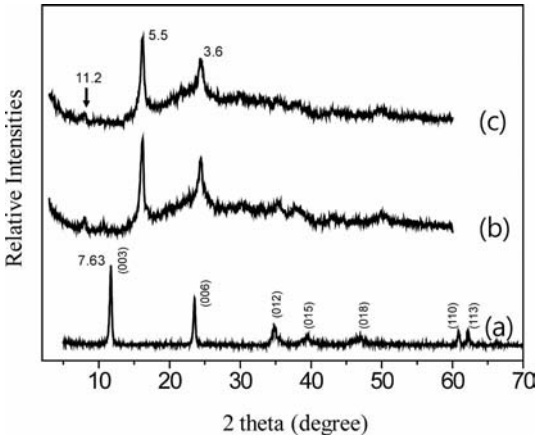

Figure 4. XRD patterns and basal spacings [Å] of (a) LDH-carbonate and (b, c) LDH-biselenite powder samples. Patterns (b) and (c) were obtained from LDH-biselenite samples prepared by ultrasound treatment in 0.5 M H_2SeO_3 in ethanol for 30 min and 2 h, respectively.

ions in the powder samples at 0.5 M acid concentration (Figure 4, b).

The LDH-biselenite samples were characterised by HRTEM, elemental mapping and chemical analyses. HRTEM (Figure 5, a) clearly indicated that the shapes and morphologies of the pristine particle were retained during anion-exchange, despite the LDH particles undergoing ultrasound treatment for over 2 h. Elemental mapping (Figure 5, b–d) showed homogeneous distributions of Mg, Al and Se, indicating that the biselenite ions were intercalated throughout the LDH. Chemical analyses for Mg, Al and Se were carried out using ICP-AES and showed that the atomic ratio of Mg/Al/Se was 1.94:1.00:0.84. The Se/Al ratio of 0.84 in the LDH-biselenite clearly indicated that the monovalent anionic species could be incorporated into the interlayer spaces of MgAl-LDH (Mg/Al ≈ 2).

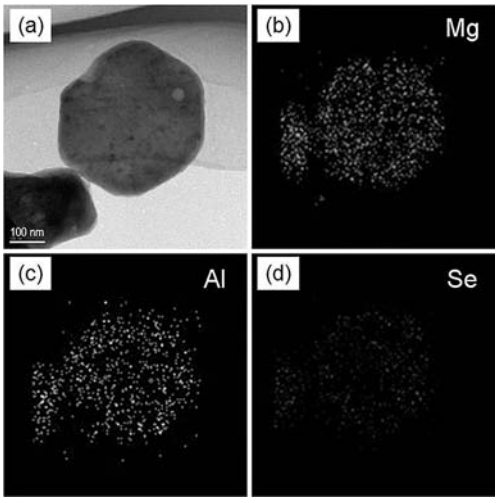

Figure 5. (a) HRTEM images and (b)–(d) elemental maps of LDH-biselenite nanocrystals. The sample was prepared by ultrasound treatment under 0.5 M H_2SeO_3 in ethanol for 2 h.

FTIR Spectroscopy of LDH-Biselenite Films

Figure 6 shows FTIR spectra for LDH-carbonate and LDH-biselenite films on Si substrates. Possible vibrational modes of free carbonate groups in the IR and Raman spectra were reported at 1064 (ν_1), 844 (ν_2), 1415 (ν_3) and 680 (ν_4) cm^{-1}.[25] The intercalated carbonates usually possess D_{3h} symmetry and lie flat between the hydroxide layers. Only three carbonate-related singlet frequencies were observed at 1355, 970 and 680 cm^{-1} in the infrared spectra.[26–28] The broad band centred at ca. 3400 cm^{-1} was assigned to overlapping stretching modes of hydroxy groups in the brucite-type layers and interlayer water molecules.[28] The intense peak at 1355 cm^{-1} for LDH-carbonate, the characteristic absorption of the antisymmetric stretching (ν_3) of interleaved carbonate, disappeared after the intercalation of biselenite (Figure 6, b).

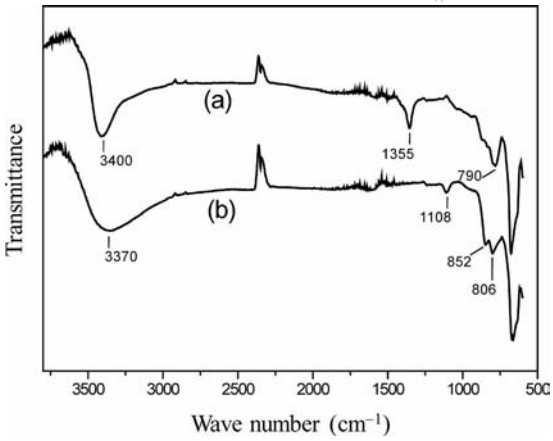

Figure 6. FTIR spectra of (a) LDH-carbonate and (b) LDH-biselenite films prepared on Si (*100*) substrates.

The spectra for LDH-biselenite also showed characteristic peaks of biselenite at 800 and 848 cm^{-1}. The absorption of selenite usually observed at 730 cm^{-1}[29] was not detected in the spectra of LDH-biselenite, implying that no selenite ions were intercalated in the LDH gallery. The very broad band centred at 3370 cm^{-1} can be ascribed to the LDH host layer and interlayer water molecules, as well as the intermolecular hydrogen bonding of biselenite. The peak at 1108 cm^{-1} of LDH-biselenite was associated with the presence of carbonate between the layers of LDH, corresponding to the ν_1 mode of the carbonate ion from lower symmetry, e.g. C_{2v},[30] which may be ascribed to the enlarged interlayer spaces after the intercalation of biselenite that could lead the carbonate ion to lie in a site of lower symmetry.

Raman Spectroscopy of LDH-Biselenite Powders

Figure 7 shows the low-frequency region of the Raman spectra of the LDH-carbonate and LDH-biselenite powders. The bands around 560 cm^{-1} for both samples were assigned to hydroxy groups mainly associated with alumin-

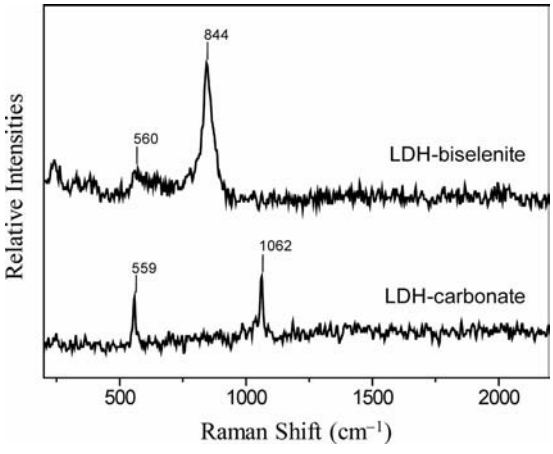

Figure 7. Raman spectra of LDH-carbonate and LDH-biselenite powder samples.

ium, though they were also influenced by magnesium coordination.[27,28] This band corresponds to the peak at 553 cm^{-1} in the FTIR spectra. In LDH-carbonate, a strong and sharp band at 1062 cm^{-1} was assigned to the interlayer carbonate ions.[27,28] The Raman spectrum of LDH-biselenite showed a very strong and sharp band at 844 cm^{-1} which is a characteristic ν_1 mode of biselenite ions.[31] No other bands attributable to selenous acid or selenite ions were observed.

Interlayer Structure of LDH-Biselenite

Selenous acid (H_2SeO_3, V = 248.11 $Å^3$)[32] is a weak diprotic acid that can exist as SeO_3^{2-}, $HSeO_3^-$ or H_2SeO_3 depending on solution pH (pK_{a1} = 2.64 and pK_{a2} = 8.4). Considering their anionic properties in the intercalation chemistry of LDH, two types of selenium anion species could be intercalated into the gallery spaces of LDHs. The spectroscopic data reported here suggest that only biselenite ions existed in the interlayer spaces of LDH-biselenite. The interlayer distances of LDH-selenite (SeO_3^{2-}) and LDH-biselenite ($HSeO_3^-$) were calculated by subtracting the LDH layer thickness, assumed to be 4.8 Å. The observed value of 8.1 Å[20] for LDH-selenite corresponds to a 3.3 Å interlayer spacing for selenite ions and the 11.5 Å observed for LDH-biselenite led to a 6.7 Å interlayer spacing for biselenite ions. This calculation suggested two different models, schematised in Figure 8. Selenite ions have C_{3v} symmetry and can be located between the layers of LDH (Figure 8, a). The biselenite ion has C_1 symmetry and a structure consisting of cyclic dimers of $HSeO_3^-$ ions joined by hydrogen bonds around their centre of symmetry (Figure 8, b), similar to the structure of $HSeO_3^-$ dimers in $NaHSeO_3$ crystals.[33]

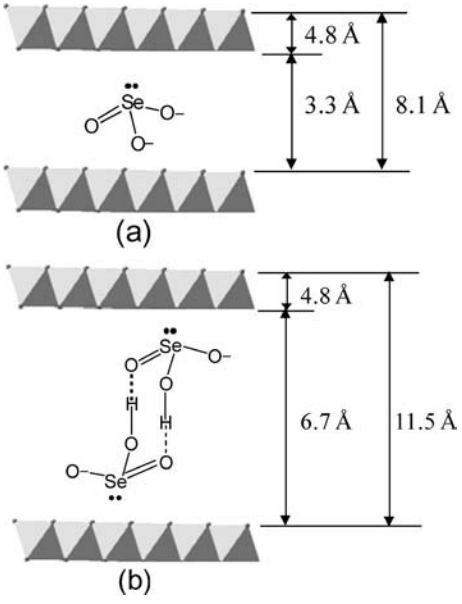

Figure 8. Interlayer structures of (a) SeO_3^{2-} and (b) $HSeO_3^-$ intercalated LDHs.

Considering the interlayer spacing of LDH-biselenite, the cyclic dimers of $HSeO_3^-$ ions were vertically arranged to the horizontal axes of the Mg-Al hydroxide layers, where the unbound oxygen atoms face one side of the inorganic layers and the centre of symmetry of the dimer was located in the centre of the interlayer space (Figure 8, b). The IR spectra of the LDH-biselenite films revealed the intermolecular hydrogen bonding of the $HSeO_3^-$ dimers because the very broad band centred around 3370 cm^{-1} has also been ascribed to intermolecular hydrogen bonding.[14–18] The present model favoured the intercalation of $HSeO_3^-$ with a cyclic dimer structure, where the dimers were vertically oriented to the horizontal axes of the Mg-Al hydroxide layers and displayed intermolecular hydrogen-bonding. Moreover, a positive surface characteristic of the MgAl-LDH-carbonate rapidly decreased over the pH range from 7 with an isoelectric point at pH 11.[34] So, this preference was possibly related to the high pK_{a2} (8.4) of selenous acid and the structural stability of the biselenite dimer. This model suggests that 2 equiv. of $HSeO_3^-$ ions could be absorbed into the LDH compared with one equiv. of SeO_3^{2-} ions, showing that the current method can be applicable to the field of a higher selenium adsorption technique.

Conclusions

A novel method of rapidly exchanging interlayer carbonate ions in LDH crystals using selenous acid in ethanol treated with ultrasound at room temperature was demonstrated with both monolayer films and powdered samples. The carbonate ions were successfully exchanged with biselenite ions at acid concentrations of 0.5 M with a 30 min reaction time for the powdered LDH-carbonate and 0.1 M with a 5 min reaction time for the thin film LDH-carbonate. The ethanol offered good solubility for the selenous acid and minimised dissolution of the LDH crystals. The intense XRD harmonics of the LDH-biselenite indicated the successful intercalation of biselenite ions with a preferred orientation. The chemical analyses and the spectroscopic evidence clearly indicate that the biselenite ions could be incorporated into the LDH gallery and the impurity carbonate remained. The basal spacing of 11.5 Å suggested cyclic dimers of interlayer anions. The morphology of the LDH-biselenite was similar to that of the pristine LDH-carbonate, indicating intercalation throughout the entire LDH crystal. Therefore, this new synthetic route could practically provide a facile intercalation method for LDH-carbonate, resulting in LDHs containing various anions with controlled crystal sizes and high crystallinity in both films and powders. The preference of $HSeO_3^-$ over SeO_3^{2-} in the present system is potentially useful to the development of high selenium adsorption techniques.

Experimental Section

Synthesis of Carbonate-Containing LDHs: $[Mg_4Al_2(OH)_{12}]CO_3 \cdot nH_2O$, LDH-carbonate, was prepared by coprecipitation.[35,36] To an aqueous solution of 0.02 M $Mg(NO_3)_2 \cdot 6H_2O$ and 0.01 M $Al(NO_3)_3 \cdot 9H_2O$ was slowly added a mixed solution of 2.0 M NaOH and 0.2 M Na_2CO_3 with vigorous stirring. The pH of the solution was adjusted to 10.0 ± 0.1 at room temperature during the titration.

The resultant precipitate was collected by centrifugation and washed three times with deionised water. Hydrothermal treatment was carried out in deionised water at 180 °C to obtain larger crystals and improve the crystallinity of the LDH-carbonate.[37] Samples were then dried at 120 °C in a convection oven. The chemical analysis for Mg and Al in LDH-carbonate was carried out using an inductively coupled plasma optical emission spectrometer (JY 38Plus, Jovin Yvon). The C and H contents were measured using an elemental analyser (EA 1000, CE Instruments) and the water content was determined from a thermo gravimetric analysis. The chemical formula of the LDH-carbonate was $[Mg_{1.94}Al_{1.00}(OH)_{6.06}](CO_3)_{0.51}\cdot 2.06\,H_2O$.

Preparation of LDH-carbonate on Si Wafers: LDH-carbonate (10 mg) was suspended in 1-butanol (20 mL) and then ultrasound was applied (95 W, 28 kHz) at room temperature in the ambient atmosphere. The Si wafer substrates were cleaned with an oxygen plasma cleaner (Harrick, 30 W), immersed in a colloidal suspension of LDH-carbonate and treated with ultrasound for 2 min. The LDH-carbonate-coated substrates were subjected to ultrasound in the solvents without LDH-carbonate for 1 min to rinse them and they were then dried at 70 °C in air.

Exchange of CO_3^{2-} with H_2SeO_3: The Si wafers with immobilised LDH-carbonate were transferred to various concentrations of H_2SeO_3 in ethanol and treated with ultrasound (95 W, 28 kHz) for 5 min at room temperature in the ambient atmosphere. They were then washed with ethanol and dried at room temperature. The LDH powder samples were prepared with ca. 100 mg of powdered LDH-carbonate being suspended in 0.5 M H_2SeO_3/ethanol and treated under similar conditions for 30 min and 2 h. The samples were collected by filtration, repeatedly washed with ethanol and dried under reduced pressure.

Characterisations: X-ray diffraction (XRD) patterns were measured using a Rigaku X-ray diffractometer, D/MAX-2000 Ultima, in θ–2θ scanning mode at 40 kV and 30 mA using Cu-K_α radiation (λ = 1.5405 Å). High-resolution transmission electron microscopy (HR-TEM) images were taken on a JEOL 300 KV (JEOL Ltd., Japan). Raman spectra were recorded at 514 nm with a Renishaw micro-Raman spectrometer. Fourier-transform infrared spectroscopy (FTIR) was undertaken on a Biorad FTS 6000 FTIR Spectrometer equipped with a high-performance DuraSampl IR II diamond accessory with an attenuated total reflectance (ATR) mode in the range of 500–4,000 cm^{-1} with 100 scans taken at 4 cm^{-1} resolution. Chemical analyses of Mg, Al and Se were carried out using an inductively coupled plasma atomic emission spectrometer (ICP-AES), JY Ultima2C (Jovin Yvon, France).

Acknowledgments

This work was funded by the National Research Laboratory (NRL) (grant number ROA-2007-000-10020-0), Korea Research Foundation (MOEHRD) (grant number KRF-2008-005-J00702), Technology Development for New and Renewable Energies Program of Korea Institute of Energy Technology Evaluation and Planning (KETEP) (grant number 2009-3021010030), Center for Human Interface Nano Technology (HINT) (grant number 2010-0015037), and The Catholic University of Korea (Research Fund 2010).

[1] L. Li, Y. Feng, Y. Li, W. Zhao, J. Shi, *Angew. Chem. Int. Ed.* **2009**, *48*, 5888–5892.
[2] S. P. Newman, W. Jones, *New J. Chem.* **1998**, *22*, 105–115.
[3] M. Meyn, K. Beneke, G. Lagaly, *Inorg. Chem.* **1990**, *29*, 5201–5207.
[4] H. Zhao, K. L. Nagy, *J. Colloid Interface Sci.* **2004**, *274*, 613–624.
[5] S. V. Prasanna, R. A. P. Rao, P. V. Kamath, *J. Colloid Interface Sci.* **2006**, *304*, 292–299.
[6] J. Das, D. Das, G. P. Dash, K. M. Parida, *J. Colloid Interface Sci.* **2002**, *251*, 26–32.
[7] A. I. Khan, D. O'Hare, *J. Mater. Chem.* **2002**, *12*, 3191–3198.
[8] F. Leroux, J.-P. Besse, *Chem. Mater.* **2001**, *13*, 3507–3515.
[9] F. Wypych, K. G. Satyanarayana, *Clay Surfaces: Fundamentals and Applications*, Elsevier, London, UK, **2004**, p. 2.
[10] N. Iyi, T. Matsumoto, Y. Kaneko, K. Kitamura, *Chem. Lett.* **2004**, *33*, 1122–1123.
[11] N. Iyi, T. Sasaki, *J. Colloid Interface Sci.* **2008**, *322*, 237–245.
[12] J. W. Boclair, P. S. Braterman, *Chem. Mater.* **1999**, *11*, 298–302.
[13] T. Hibino, A. Tsunashima, *Chem. Mater.* **1997**, *9*, 2082–2089.
[14] J. H. Lee, S. W. Rhee, H. J. Nam, D. Y. Jung, *Adv. Mater.* **2009**, *21*, 546–549.
[15] J. H. Lee, S. W. Rhee, H. J. Nam, D. Y. Jung, *J. Am. Chem. Soc.* **2007**, *129*, 3522–3523.
[16] J. H. Lee, S. W. Rhee, H. J. Nam, D. Y. Jung, *Chem. Mater.* **2006**, *18*, 4740–4746.
[17] J. H. Lee, S. W. Rhee, H. J. Nam, D. Y. Jung, *Chem. Mater.* **2004**, *16*, 3774–3779.
[18] J. H. Lee, S. W. Rhee, H. J. Nam, D. Y. Jung, *Chem. Commun.* **2003**, 2740–2741.
[19] F. Kooli, W. Jones, *J. Mater. Sci. Lett.* **1997**, *16*, 27–29.
[20] X. Hou, R. J. Kirkpatrick, *Chem. Mater.* **2000**, *12*, 1890–1897.
[21] A. M. Fogg, V. M. Green, H. G. Harvey, D. O' Hare, *Adv. Mater.* **1999**, *11*, 1466–1469.
[22] M. Borja, P. K. Dutta, *J. Phys. Chem.* **1992**, *96*, 5434–5444.
[23] P. Beaudot, M. E. de Roy, J. P. Besse, *J. Solid State Chem.* **2001**, *161*, 332–340.
[24] P. Beaudot, M. E. de Roy, J. P. Besse, *J. Solid State Chem.* **2004**, *177*, 2691–2698.
[25] K. Nakamoto, *Infrared and Raman Spectra of Inorganic and Coordination Compounds*, Mineralogical Society, England, **1974**.
[26] M. Jitianu, M. Bălăsoiu, R. Marchidan, M. Zaharescu, D. Crisan, M. Craiu, *Int. J. Inorg. Mater.* **2000**, *2*, 287–300.
[27] W. Kagunya, R. Baddour-Hadjean, F. Kooli, W. Jones, *Chem. Phys.* **1998**, *236*, 225–234.
[28] J. T. Kloprogge, R. L. Frost, *J. Solid State Chem.* **1999**, *146*, 506–515.
[29] B. H. Torrie, *Can. J. Phys.* **1973**, *51*, 610–615.
[30] K. Fuda, N. Kuda, S. Kawai, T. Matsunaga, *Chem. Lett.* **1993**, 777–778.
[31] G. E. Walrafen, *J. Chem. Phys.* **1962**, *36*, 90–93.
[32] The geometry was optimised by using an ab initio method (using a STO-3G parameter). The molecular volume was calculated using the quantitative structure–activity relationship (QSAR) properties of HyperChem v. 7.52. Within the selenous acid molecule, the Se–O bond has a length of 1.64 Å and the Se–OH bonds have lengths of 1.74 and 1.76 Å. The average O···O distance is 2.66 Å. Assuming van der Waals radii of oxygen, hydrogen and selenium of 1.52, 1.09 and 1.90 Å, respectively, the selenous acid has a length of 4.54 Å and a width of 5.70 Å.
[33] A. R. Lim, S. W. Jang, J.-H. Chang, *Solid State Nucl. Magn. Reson.* **2007**, *31*, 124–130.
[34] O. C. Wilson Jr., T. Olorunyolemi, A. Jaworski, L. Borum, D. Young, A. Siriwat, E. Dickens, C. Oriakhi, M. Lerner, *Appl. Clay Sci.* **1999**, *15*, 265–279.
[35] S. Miyata, *Clays Clay Miner.* **1983**, *31*, 305–311.
[36] S. Miyata, A. Okada, *Clays Clay Miner.* **1977**, *25*, 14–25.
[37] L. Hickey, J. L. Kloprogge, R. L. Frost, *J. Mater. Sci.* **2000**, *35*, 4347–4355.

Received: March 16, 2011
Published Online: June 28, 2011

